3

NUCLEAR PROPERTIES

Like many systems governed by the laws of quantum mechanics, the nucleus is a somewhat enigmatic and mysterious object whose properties are much more difficult to characterize than are those of macroscopic objects. The list of instructions needed to build an exact replica of a French colonial house or a '57 Chevy is relatively short; the list of instructions necessary to characterize all of the mutual interactions of the 50 nucleons in a medium weight nucleus could contain as many as 50! or about 10^{64} terms! We must therefore select a different approach and try to specify the overall characteristics of the entire nucleus. Are there a few physical properties that can be listed to give an adequate description of any nucleus?

To a considerable extent, we can describe a nucleus by a relatively small number of parameters: electric charge, radius, mass, binding energy, angular momentum, parity, magnetic dipole and electric quadrupole moments, and energies of excited states. These are the *static properties* of nuclei that we consider in this chapter. In later chapters we discuss the *dynamic properties* of nuclei, including decay and reaction probabilities. To understand these static and dynamic properties in terms of the interaction between individual nucleons is the formidable challenge that confronts the nuclear physicist.

3.1 THE NUCLEAR RADIUS

Like the radius of an atom, the radius of a nucleus is not a precisely defined quantity; neither atoms nor nuclei are solid spheres with abrupt boundaries. Both the Coulomb potential that binds the atom and the resulting electronic charge distribution extend to infinity, although both become negligibly small at distances far beyond the atomic radius (10^{-10} m). What is required is an "operational definition" of what we are to take as the value of the atomic radius. For instance, we might define the atomic radius to be the largest mean radius of the various electronic states populated in an atom. Such a property would be exceedingly difficult to measure, and so more practical definitions are used, such as the spacing between atoms in ionic compounds containing the atom of interest. This also leads to some difficulties since we obtain different radii for an atom when it is in different compounds or in different valence states.

For nuclei, the situation is better in some aspects and worse in others. As we will soon discuss, the density of nucleons and the nuclear potential have a similar spatial dependence—relatively constant over short distances beyond which they drop rapidly to zero. It is therefore relatively natural to characterize the nuclear shape with two parameters: the mean radius, where the density is half its central value, and the "skin thickness," over which the density drops from near its maximum to near its minimum. (In Section 5 of this chapter, we discuss a third parameter, which is necessary to characterize nuclei whose shape is not spherical.)

The problems we face result from the difficulty in determining just what it is that the distribution is describing; the radius that we measure depends on the kind of experiment we are doing to measure the nuclear shape. In some experiments, such as high-energy electron scattering, muonic X rays, optical and X-ray isotope shifts, and energy differences of mirror nuclei, we measure the Coulomb interaction of a charged particle with the nucleus. These experiments would then determine the *distribution of nuclear charge* (primarily the distribution of protons but also involving somewhat the distribution of neutrons, because of their internal structure). In other experiments, such as Rutherford scattering, α decay, and pionic X rays, we measure the strong nuclear interaction of nuclear particles, and we would determine the distribution of nucleons, called the *distribution of nuclear matter*.

The Distribution of Nuclear Charge

Our usual means for determining the size and shape of an object is to examine the radiation scattered from it (which is, after all, what we do when we look at an object or take its photograph). To see the object and its details, the wavelength of the radiation must be smaller than the dimensions of the object; otherwise the effects of diffraction will partially or completely obscure the image. For nuclei, with a diameter of about 10 fm, we require $\lambda \lesssim 10$ fm, corresponding to $p \gtrsim 100$ MeV/c. Beams of electrons with energies 100 MeV to 1 GeV can be produced with high-energy accelerators, such as the Stanford linear accelerator, and can be analyzed with a precise spectrometer to select only those electrons that are elastically scattered from the selected nuclear target. Figure 3.1 shows an example of the results of such an experiment. The first minimum in the diffractionlike pattern can clearly be seen; for diffraction by a circular disk of diameter D, the first minimum should appear at $\theta = \sin^{-1}(1.22\lambda/D)$, and the resulting estimates for the nuclear radii are 2.6 fm for ^{16}O and 2.3 fm for ^{12}C. These are, however, only rough estimates because potential scattering is a three-dimensional problem only approximately related to diffraction by a two-dimensional disk.

Figure 3.2 shows the results of elastic scattering from a heavy nucleus, ^{208}Pb. Several minima in the diffractionlike pattern can be seen. These minima do not fall to zero like diffraction minima seen with light incident on an opaque disk, because the nucleus does not have a sharp boundary.

Let us try to make this problem more quantitative. The initial electron wave function is of the form $e^{ik_i \cdot r}$, appropriate for a free particle of momentum $p_i = \hbar k_i$. The scattered electron can also be regarded as a free particle of momentum $p_f = \hbar k_f$ and wave function $e^{ik_f \cdot r}$. The interaction $V(r)$ converts the initial wave into the scattered wave, and according to Equation 2.80 the probabil-
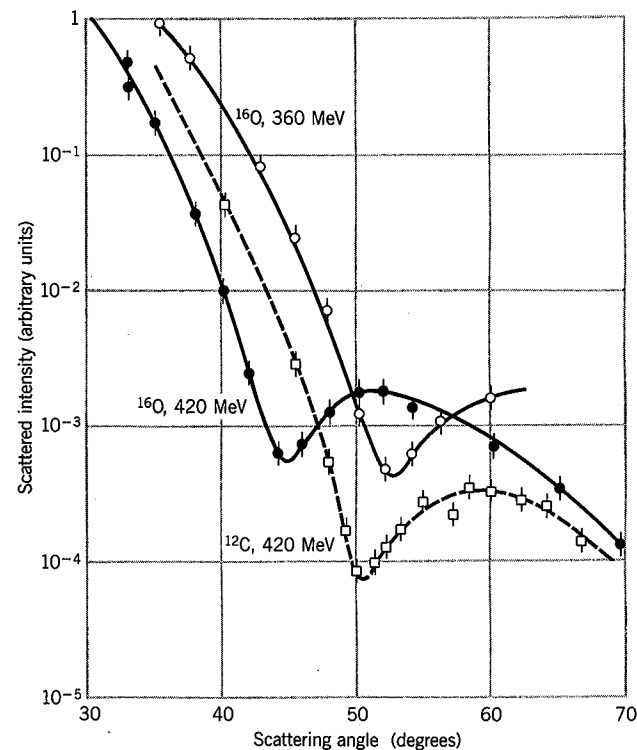
Figure 3.1 Electron scattering from ^{16}O and ^{12}C. The shape of the cross section is somewhat similar to that of diffraction patterns obtained with light waves. The data come from early experiments at the Stanford Linear Accelerator Center (H. F. Ehrenberg et al., *Phys. Rev.* **113**, 666 (1959)).

Figure 3.2 Elastic scattering of electrons from ^{208}Pb. Note the different vertical and horizontal scales for the two energies. This also shows diffractionlike behavior, but lacks sharp minima. (J. Heisenberg et al., *Phys. Rev. Lett.* **23**, 1402 (1969).)

ity for the transition will be proportional to the square of the quantity

$$F(k_i, k_f) = \int \psi_f^* V(r) \psi_i \, dv \qquad (3.1)$$

$$F(q) = \int e^{iq \cdot r} V(r) \, dv \qquad (3.2)$$

apart from a normalization constant, which is chosen so that $F(0) = 1$. Here $q = k_i - k_f$, which is essentially the momentum change of the scattered electron. The interaction $V(r)$ depends on the nuclear charge density $Ze\rho_e(r')$, where r' is a coordinate describing a point in the nuclear volume and ρ_e gives the distribution of nuclear charge. That is, as indicated in Figure 3.3, an electron located at r feels a potential energy due to the element of charge dQ located at r':

$$dV = -\frac{e \, dQ}{4\pi\epsilon_0 |r - r'|}$$

$$= -\frac{Ze^2 \rho_e(r') \, dv'}{4\pi\epsilon_0 |r - r'|} \qquad (3.3)$$

To find the complete interaction energy $V(r)$, we sum over all of the contribu-

tions dQ within the nucleus:

$$V(r) = -\frac{Ze^2}{4\pi\epsilon_0} \int \frac{\rho_e(r') \, dv'}{|r - r'|} \qquad (3.4)$$

Writing $q \cdot r = qr \sin\theta$ in Equation 3.2 and integrating over r, the properly normalized result is

$$F(q) = \int e^{iq \cdot r'} \rho_e(r') \, dv' \qquad (3.5)$$

and if $\rho_e(r')$ depends only on the magnitude r' (not on θ' or ϕ') we obtain

$$F(q) = \frac{4\pi}{q} \int \sin qr' \rho_e(r') r' \, dr' \qquad (3.6)$$

This quantity is a function of q, the magnitude of q. Since we originally assumed that the scattering was elastic, then $|p_i| = |p_f|$ and q is merely a function of the scattering angle α between p_i and p_f; a bit of vector manipulation shows $q = (2p/\hbar) \sin \alpha/2$ where p is the momentum of the electron. Measuring the scattering probability as a function of the angle α then gives us the dependence
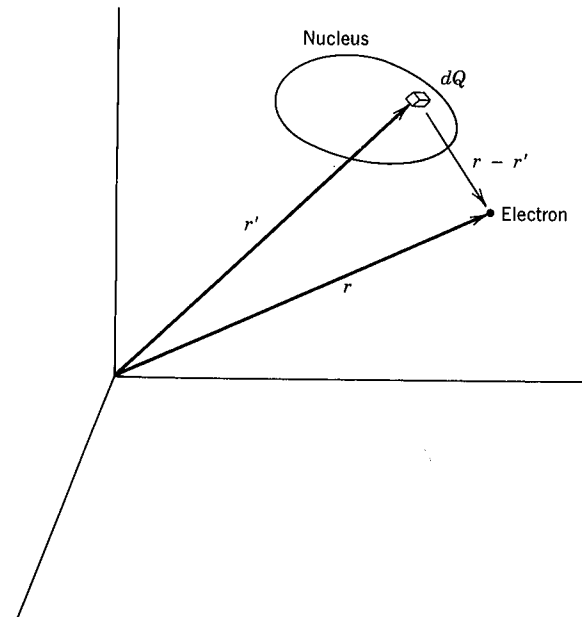
Figure 3.3 The geometry of scattering experiments. The origin of coordinates is located arbitrarily. The vector **r'** locates an element of charge dQ within the nucleus, and the vector **r** defines the position of the electron.

of Equation 3.6 on q. The quantity $F(q)$ is known as a form factor, and the numerical inversion of Equation 3.6, actually an inverse Fourier transformation, then gives us $\rho_e(r')$.

The results of this procedure for several different nuclei are shown in Figure 3.4. One remarkable conclusion is obvious—the central nuclear charge density is nearly the same for all nuclei. Nucleons do not seem to congregate near the center of the nucleus, but instead have a fairly constant distribution out to the surface. (The conclusion from measurements of the nuclear matter distribution is the same.) Thus *the number of nucleons per unit volume is roughly constant*:

$$\frac{A}{\frac{4}{3}\pi R^3} \sim \text{constant} \tag{3.7}$$

where R is the mean nuclear radius. Thus $R \propto A^{1/3}$, and defining the proportionality constant R_0 gives

$$R = R_0 A^{1/3} \tag{3.8}$$

From electron scattering measurements, such as those in Figure 3.4, it is concluded that $R_0 \simeq 1.2$ fm. These measurements give the most detailed descriptions of the complete nuclear charge distribution.

Figure 3.4 also shows how diffuse the nuclear surface appears to be. The charge density is roughly constant out to a certain point and then drops relatively slowly to zero. The distance over which this drop occurs is nearly independent of the size of the nucleus, and is usually taken to be constant. We define the *skin*
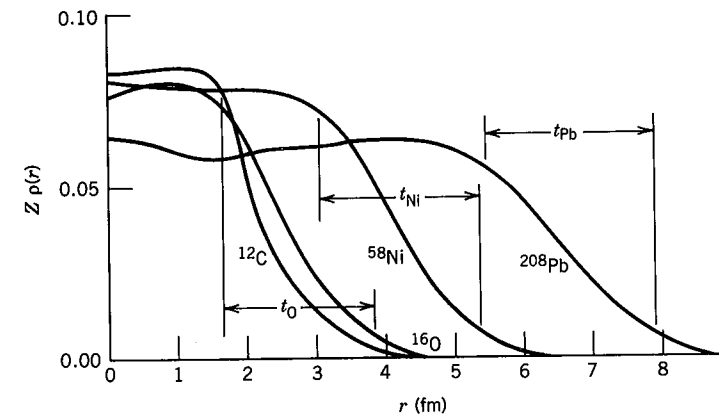
Figure 3.4 The radial charge distribution of several nuclei determined from electron scattering. The skin thickness t is shown for O, Ni, and Pb; its value is roughly constant at 2.3 fm. The central density changes very little from the lightest nuclei to the heaviest. These distributions were adapted from R. C. Barrett and D. F. Jackson, *Nuclear Sizes and Structure* (Oxford: Clarendon, 1977), which gives more detail on methods of determining $\rho(r)$.

thickness parameter t as the distance over which the charge density falls from 90% of its central value to 10%. The value of t is approximately 2.3 fm.

Figure 3.5 shows a more quantitative determination of the relationship between the nuclear radius and mass number, based on electron scattering results. The root mean square (rms) radius, $\langle r^2 \rangle^{1/2}$, is deduced directly from the distribution of scattered electrons; for a uniformly charged sphere $\langle r^2 \rangle = \frac{3}{5} R^2$, where R is the radius of the sphere. Figure 3.5 shows that the dependence of R on $A^{1/3}$ is approximately valid over the range from the lightest to the heaviest nuclei. From the slope of the line, we deduce $R_0 = 1.23$ fm.

The nuclear charge density can also be examined by a careful study of atomic transitions. In solving the Schrödinger equation for the case of the atom with a single electron, it is always assumed that the electron feels the Coulomb attraction of a *point* nucleus, $V(r) = -Ze^2/4\pi\epsilon_0 r$. Since real nuclei are not points, the electron wave function can penetrate to $r < R$, and thus the electron spends part of its time *inside* the nuclear charge distribution, where it feels a very different interaction. In particular, as $r \to 0$, $V(r)$ will not tend toward infinity for a nucleus with a nonzero radius. As a rough approximation, we can assume the nucleus to be a uniformly charged sphere of radius R, for which the potential energy of the electron for $r \leq R$ is

$$V'(r) = -\frac{Ze^2}{4\pi\epsilon_0 R}\left\{\frac{3}{2} - \frac{1}{2}\left(\frac{r}{R}\right)^2\right\} \tag{3.9}$$

while for $r \geq R$, the potential energy has the point–nucleus form.

The total energy E of the electron in a state ψ_n of a point nucleus depends in part on the expectation value of the potential energy

$$\langle V \rangle = \int \psi_n^* V \psi_n \, dv \tag{3.10}$$
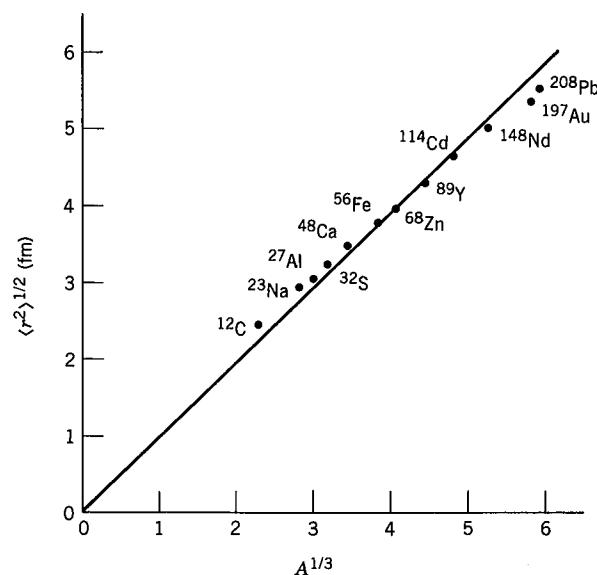
Figure 3.5 The rms nuclear radius determined from electron scattering experiments. The slope of the straight line gives $R_0 = 1.23$ fm. (The line is not a true fit to the data points, but is forced to go through the origin to satisfy the equation $R = R_0 A^{1/3}$.) The error bars are typically smaller than the size of the points (± 0.01 fm). More complete listings of data and references can be found in the review of C. W. de Jager et al., *Atomic Data and Nuclear Data Tables* **14**, 479 (1974).

where V is the point–nucleus Coulomb potential energy. If we assume (as a first approximation) that changing from a point nucleus to a uniformly charged spherical nucleus does not significantly change the electronic wave function ψ_n, then the energy E' of the electron in a state of a uniformly charged spherical nucleus depends on the expectation value of the potential V':

$$\langle V' \rangle = \int_{r<R} \psi_n^* V' \psi_n \, dv + \int_{r>R} \psi_n^* V \psi_n \, dv \qquad (3.11)$$

where the second integral involves only the $1/r$ potential energy. The effect of the spherical nucleus is thus to change the energy of the electronic states, relative to the point–nucleus value, by $\Delta E = E' - E = \langle V' \rangle - \langle V \rangle$; the latter step follows directly from our assumption that the wave functions are the same, in which case the kinetic energy terms in E and E' are identical. Using the 1s hydrogenic wave function from Table 2.5, we find

$$\Delta E = \frac{e^2}{4\pi\epsilon_0} \frac{4Z^4}{a_0^3} \int_0^R e^{-2Zr/a_0} \left\{ \frac{1}{r} - \frac{3}{2R} + \frac{1}{2} \frac{r^2}{R^3} \right\} r^2 \, dr \qquad (3.12)$$

The exponential factor in the integrand is nearly unity, because $R/a_0 \simeq 10^{-5}$, and evaluating the remaining terms gives

$$\Delta E = \frac{2}{5} \frac{Z^4 e^2}{4\pi\epsilon_0} \frac{R^2}{a_0^3} \qquad (3.13)$$

This ΔE is the difference between the energy of the 1s state in an atom with a "point" nucleus and the 1s energy in an atom with a uniformly charged nucleus of radius R. The latter is a fair approximation to real nuclei (as suggested by Figure 3.4); if we could only find a supply of atoms with "point" nuclei we could measure ΔE and deduce R! Since no such nuclei exist, the next best strategy would be to determine E' from measurement (from K X rays, for example) and to calculate the point–nucleus value E from the 1s atomic wave function. Unfortunately, the atomic wave functions are not known with sufficient precision to do this—ΔE is a very small difference, perhaps 10^{-4} of E, and the simple hydrogenlike 1s wave functions are not good enough to calculate E to a precision of 1 part in 10^4 (relativistic effects and the presence of other electrons are two factors that also influence the 1s energy). Thus a single measurement of the energy of a K X ray cannot be used to deduce the nuclear radius.

Let's instead measure and compare the K X-ray energies (resulting from 2p → 1s electronic transitions) in two neighboring isotopes of mass numbers A and A'. Letting $E_K(A)$ and $E_K(A')$ represent the observed K X-ray energies, we have

$$E_K(A) - E_K(A') = E_{2p}(A) - E_{1s}(A) - E_{2p}(A') + E_{1s}(A') \qquad (3.14)$$

If we assume that the 2p energy difference is negligible (recall from Chapter 2 that p-electron wave functions vanish at $r = 0$), the remaining 1s energy difference reduces to the difference between the ΔE values of Equation 3.13, because $E_{1s} \equiv E' = E + \Delta E$ and the "point" nucleus values E would be the same for the isotopes A and A'. Thus

$$E_K(A) - E_K(A') = \Delta E(A') - \Delta E(A)$$

$$= -\frac{2}{5} \frac{Z^4 e^2}{4\pi\epsilon_0} \frac{1}{a_0^3} R_0^2 (A^{2/3} - A'^{2/3}) \qquad (3.15)$$

The quantity $E_K(A) - E_K(A')$ is called the K X-ray *isotope shift*, and a plot against $A^{2/3}$ of a sequence of isotope shifts of different isotopes A all compared with the same reference A' should give a straight line from whose slope we could deduce R_0. Figure 3.6 is an example of such a plot for some isotopes of Hg. The agreement with the $A^{2/3}$ dependence is excellent. The slope, however, does not give a reasonable value of R_0, because the 1s wave function used in Equation 3.12 is not a very good representation of the true 1s wave function. The calculated K X-ray energies, for example, are about 10% lower than the observed values. Detailed calculations that treat the 1s electron relativistically and take into account the effect of other electrons give a more realistic relationship between the slope of Figure 3.6 and the value of R_0. The resulting values are in the range of 1.2 fm, in agreement with the results of electron scattering experiments.
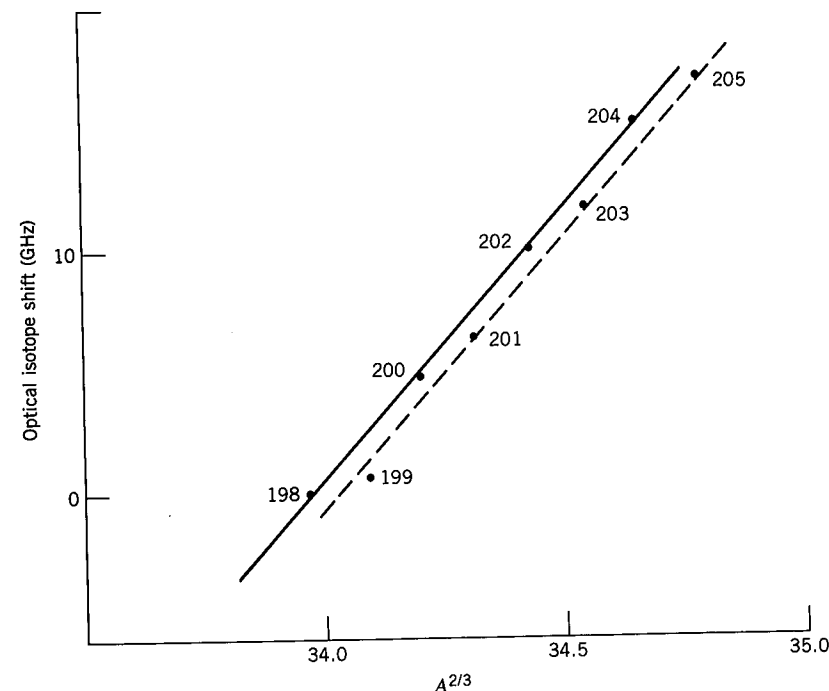
It is also possible to measure isotope shifts for the *optical* radiations in atoms (those transitions among the outer electronic shells that produce visible light). Because these electronic orbits lie much further from the nucleus than the 1s orbit, their wave functions integrated over the nuclear volume, as in Equation 3.12, give much smaller shifts than we obtain for the inner 1s electrons. In Chapter 2 we showed that s states ($\ell = 0$ wave functions) give nonzero limits on
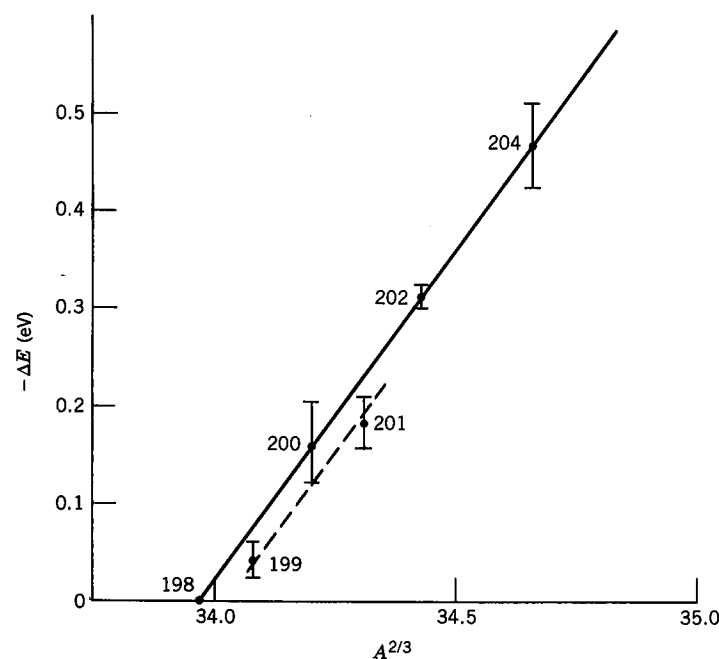
Figure 3.6 K X-ray isotope shifts in Hg. The energy of the K X ray in Hg is about 100 keV, so the relative isotope shift is of the order of 10^{-6}. The data show the predicted dependence on $A^{2/3}$. There is an "odd-even" shift in radius of odd-mass nuclei relative to their even-A neighbors, brought about by the orbit of the odd particle. For this reason, odd-A isotopes must be plotted separately from even-A isotopes. Both groups, however, show the $A^{2/3}$ dependence. The data are taken from P. L. Lee et al., *Phys. Rev. C* **17**, 1859 (1978).

Figure 3.7 Optical isotope shifts in Hg isotopes from 198 to 205, measured relative to 198. These data were obtained through laser spectroscopy; the experimental uncertainties are about ±1%. The optical transition used for these measurements has a wavelength of 253.7 nm, and the isotope shift is therefore about one part in 10^7. Compare these results with Figure 3.6. Data taken from J. Bonn et al., *Z. Phys. A* **276**, 203 (1976).

ψ at small r. If the optical transitions involve s states, their isotope shifts can be large enough to be measured precisely, especially using modern techniques of laser interferometry. Figure 3.7 shows an example of optical shifts in Hg isotopes; again the expected $A^{2/3}$ dependence is consistent with the data. Measurements across a large range of nuclei are consistent with $R_0 = 1.2$ fm.

These effects of the nuclear size on X-ray and optical transitions are very small, about 10^{-4} to 10^{-6} of the transition energy. The reason these effects are so small has to do with the difference in scale of 10^4 between the Bohr radius a_0 and the nuclear radius R. For integrals of the form of Equation 3.12 to give large effects, the atomic wave function should be large at values of r near R, but instead the atomic wave functions are large near $r = a_0/Z$, which is far greater than R. We can improve on this situation by using a *muonic atom*. The muon is a particle identical to the electron in all characteristics except its mass, which is 207 times the electronic mass. Since the Bohr radius depends inversely on the mass, the muonic orbits have 1/207 the radius of the corresponding electronic orbits. In fact, in a heavy nucleus like Pb, the muonic 1s orbit has its mean radius *inside* the nuclear radius R; the effect of the nuclear size is a factor of 2 in the transition energies, a considerable improvement over the factor of 10^{-4} to 10^{-6} in electronic transitions.

Muons are not present in ordinary matter, but must be made artificially using large accelerators that produce intense beams of π mesons. The π mesons then decay rapidly (10^{-8} s) to muons. (The properties of muons and π mesons are discussed in Chapters 17 and 18.) Beams of the resulting muons are then focused onto a suitably chosen target; atoms of the target capture the muons into orbits similar to electronic orbits. Initially the muon is in a state of very high principal quantum number n, and as the muon cascades down toward its 1s ground state, photons are emitted, in analogy with the photons emitted in electronic transitions between energy levels. The energy levels of atomic hydrogen depend directly on the electronic mass; we therefore expect the muonic energy levels and transition energies to be 207 times their electronic counterparts. Since ordinary K X rays are in the energy range of tens of keV, muonic K X rays will have energies of a few MeV. Figure 3.8 shows some typical muonic K X rays; the isotope shift is large compared with the isotope shift of electronic K X rays, which is typically 10^{-2} eV per unit change in A.

In contrast to the case with electronic K X rays, where uncertainties in atomic wave functions made it difficult to interpret the isotope shifts, we can use the observed muonic X-ray energies directly to compute the parameters of the nuclear charge distribution. Figure 3.9 shows the deduced rms radii, based once
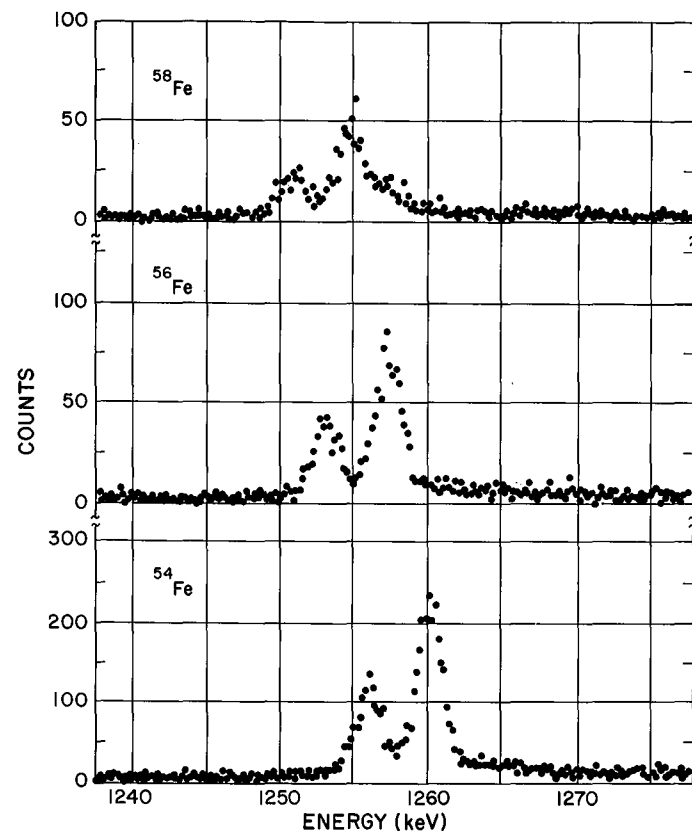
Figure 3.8 The muonic K X rays in some Fe isotopes. The two peaks show the $2p_{3/2}$ to $1s_{1/2}$ and $2p_{1/2}$ to $1s_{1/2}$ transitions, which have relative intensities in the ratio 2 : 1 determined by the statistical weight $(2j + 1)$ of the initial state. The isotope shift can clearly be seen as the change in energy of the transitions. The effect is about 0.4%, which should be compared with the 10^{-6} effect obtained with electronic K X rays (Figure 3.6). From E. B. Shera et al., *Phys. Rev. C* **14**, 731 (1976).

again on the model of the uniformly charged sphere. The data are roughly consistent with $R_0 A^{1/3}$, with $R_0 = 1.25$ fm.

Yet another way to determine the nuclear charge radius is from direct measurement of the Coulomb energy differences of nuclei. Consider, for example, $^3_1H_2$ and $^3_2He_1$. To get from ^3He to ^3H, we must change a proton into a neutron. As we discuss in Chapter 4, there is strong evidence which suggests that the *nuclear* force does not distinguish between protons and neutrons. Changing a proton into a neutron should therefore not affect the *nuclear* energy of the three-nucleon system; only the Coulomb energy should change, because the two protons in ^3He experience a repulsion that is not present in ^3H. The energy difference between ^3He and ^3H is thus a measure of the Coulomb energy of the second proton, and the usual formula for the Coulomb repulsion energy can be used to calculate the distance between the protons and thus the size of the nucleus.
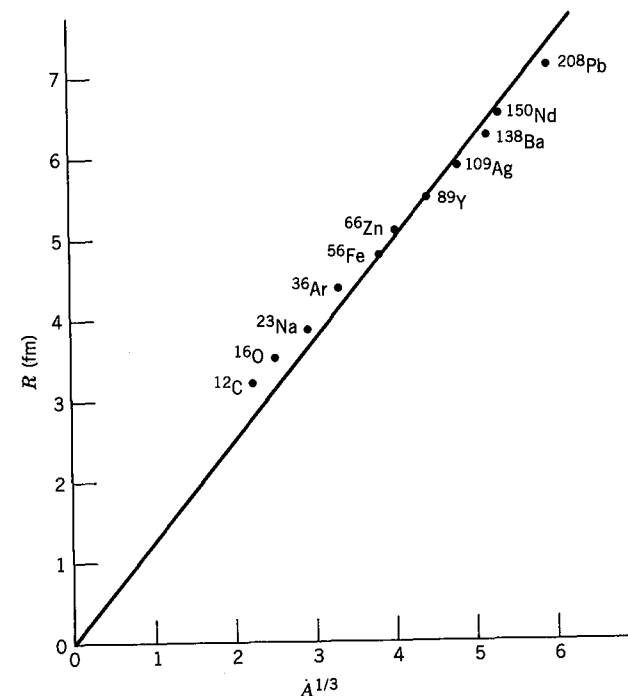
Figure 3.9 The mean nuclear radius determined from muonic X-ray measurements. As in Figure 3.5, the data depend roughly linearly on $A^{1/3}$ (again forcing the line to go through the origin). The slope of the line gives $R_0 = 1.25$ fm. The data are taken from a review of muonic X-ray determinations of nuclear charge distributions by R. Engfer et al., *Atomic Data and Nuclear Data Tables* **14**, 509 (1974).

Consider now a more complex nucleus, such as $^{238}_{92}U_{146}$. If we try to change a proton to a neutron we now have a very different circumstance, because the 92nd proton would become the 147th neutron. Because neutrons and protons each must obey the Pauli principle, the orbital of the 92nd proton will differ from the orbital of the 147th neutron, and in general it is not possible to calculate this effect to sufficient accuracy to be able to extract the Coulomb energy. The situation is resolved if we choose a case (as with ^3He–^3H) in which no change of orbital is involved, that is, in which the number of the last proton that makes the change is identical to the number of the last neutron after the change. The Z of the first nucleus must equal the N of the second (and thus the N of the first equals the Z of the second). Such pairs of nuclei are called *mirror nuclei* because one is changed into the other by "reflecting" in a mirror that exchanges protons and neutrons. Examples of such pairs of mirror nuclei are $^{13}_7N_6$ and $^{13}_6C_7$, or $^{39}_{20}Ca_{19}$ and $^{39}_{19}K_{20}$.

The Coulomb energy of a uniformly charged sphere of radius R is

$$E_c = \frac{3}{5} \frac{1}{4\pi\epsilon_0} \frac{Q^2}{R} \tag{3.16}$$

where Q is the total charge of the sphere. The difference in Coulomb energy

between the mirror pairs is thus

$$\Delta E_c = \frac{3}{5} \frac{e^2}{4\pi\epsilon_0 R}\left[Z^2 - (Z-1)^2\right]$$

$$= \frac{3}{5} \frac{e^2}{4\pi\epsilon_0 R}(2Z - 1) \qquad (3.17)$$

Since Z represents the nucleus of higher atomic number, the N of that nucleus must be $Z - 1$, and so $A = 2Z - 1$. With $R = R_0 A^{1/3}$,

$$\Delta E_c = \frac{3}{5} \frac{e^2}{4\pi\epsilon_0 R_0}A^{2/3} \qquad (3.18)$$

These Coulomb energy differences can be directly measured in two ways. One of the nuclei in the pair can decay to the other through *nuclear β decay*, in which a proton changes into a neutron with the emission of a positive electron (positron). The maximum energy of the positron is a measure of the energy difference between the nuclei. A second method of measuring the energy difference is through nuclear reactions; for example, when a nucleus such as ^{11}B is bombarded with protons, occasionally a neutron will be emitted leaving the residual nucleus ^{11}C. The minimum proton energy necessary to cause this reaction is a measure of the energy difference between ^{11}B and ^{11}C. (We discuss β decay in Chapter 9 and reaction kinematics in Chapter 11.) The measured energy differences are plotted against $A^{2/3}$ in Figure 3.10. As expected from Equation 3.18, the dependence is very nearly linear. The slope of the line gives $R_0 = 1.22$ fm.
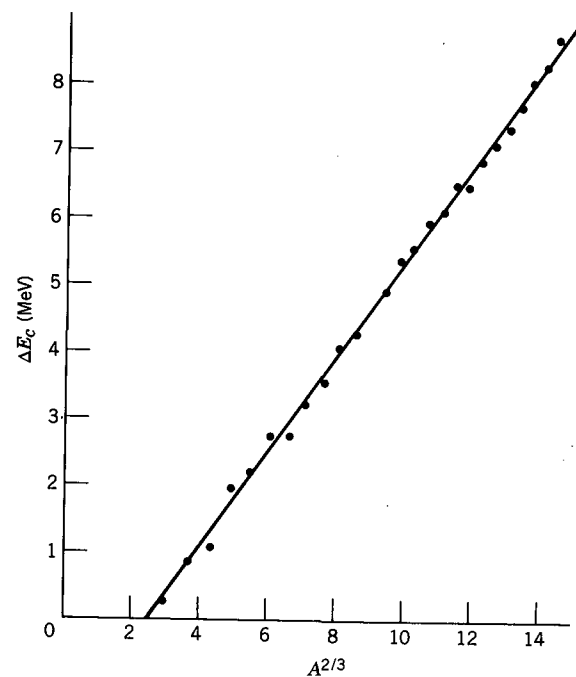
Figure 3.10 Coulomb energy differences of mirror nuclei. The data show the expected $A^{2/3}$ dependence, and the slope of the line gives $R_0 = 1.22$ fm.

Even though these measurements of the nuclear charge radius use very different techniques, they all give essentially the same results: the nuclear radius varies with mass number as $R_0 A^{1/3}$, with $R_0 = 1.2 - 1.25$ fm.

The Distribution of Nuclear Matter

An experiment that involves the nuclear force between two nuclei will often provide a measure of the nuclear radius. The determination of the spatial variation of the force between nuclei enables the calculation of the nuclear radii. In this case the radius is characteristic of the *nuclear*, rather than the *Coulomb*, force; these radii therefore reflect the distribution of all nucleons in a nucleus, not only the protons.

As an example of a measurement that determines the size of the nuclear matter distribution, we consider an experiment in which a ^{4}He nucleus (α particle) is scattered from a much heavier target of ^{197}Au. If the separation between the two nuclei is always greater than the sum of their radii, each is always beyond the range of the other's nuclear force, so only the Coulomb force acts. (This situation is known as Rutherford scattering and is discussed in Chapter 11.) The probability for scattering at a certain angle depends on the energy of the incident particle exactly as predicted by the Rutherford formula, when the energy of the incident particle is below a certain value. As the energy of the incident α particle is increased, the Coulomb repulsion of the nuclei is overcome and they may approach close enough to allow the nuclear force to act. In this case the Rutherford formula no longer holds. Figure 3.11 shows an example of this effect.

For another example, we consider the form of radioactive decay in which an α particle is emitted from the nucleus (see Chapter 8 for a complete discussion of α decay). The α particle must escape the nuclear potential and penetrate a Coulomb potential barrier, as indicated in Figure 3.12. The α decay probabilities can be calculated from a standard barrier-penetration approach using the Schrödinger equation. These calculated values depend on the nuclear matter radius R, and comparisons with measured decay probabilities permit values of R to be deduced.

A third method for determining the nuclear matter radius is the measurement of the energy of π-mesic X rays. This method is very similar to the muonic X-ray technique discussed above for measuring the charge radius. The difference between the two techniques results from differences between muons and π mesons: the muons interact with the nucleus through the Coulomb force, while the π mesons interact with the nucleus through the nuclear and the Coulomb forces. Like the muons, the negatively charged π mesons cascade through electronlike orbits and emit photons known as π-mesic X rays. When the π-meson wave functions begin to overlap with the nucleus, the energy levels are shifted somewhat from values calculated using only the Coulomb interaction. In addition, the π mesons can be directly absorbed into the nucleus, especially from the inner orbits; thus there are fewer X-ray transitions among these inner levels. The "disappearance rate" of π mesons gives another way to determine the nuclear radius.

All of these effects could in principle be used as a basis for deducing the nuclear radius. However, the calculations are very sensitive to the exact onset of
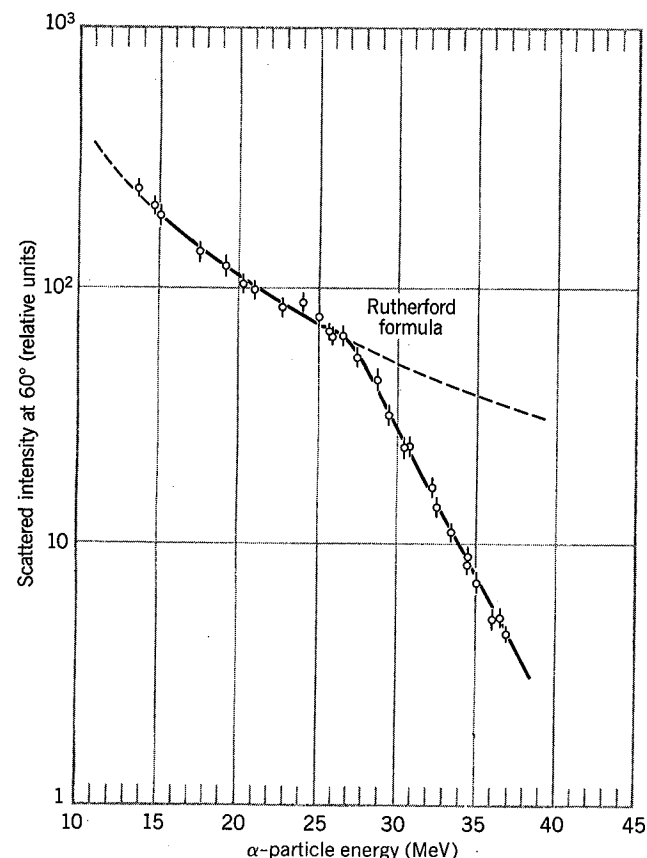
Figure 3.11 The breakdown of the Rutherford scattering formula. When the incident α particle gets close enough to the target Pb nucleus so that they can interact through the nuclear force (in addition to the Coulomb force that acts when they are far apart) the Rutherford formula no longer holds. The point at which this breakdown occurs gives a measure of the size of the nucleus. Adapted from a review of α particle scattering by R. M. Eisberg and C. E. Porter, *Rev. Mod. Phys.* **33**, 190 (1961).

overlap between the probe particle and the nuclear matter distribution. For these calculations it is therefore very wrong to use the "uniform sphere" model of assuming a constant density out to R and zero beyond R. We should instead use a distribution, such as those of Figure 3.4, with a proper tail beyond the mean radius.

We will not go into the details of the calculations, which are far more complicated than our previous calculations of the charge radius. We merely give the result, which may seem a bit surprising: *the charge and matter radii of nuclei are nearly equal, to within about 0.1 fm.* Both show the $A^{1/3}$ dependence with $R_0 \simeq 1.2$ fm. Because heavy nuclei have about 50% more neutrons than protons, we might have expected the neutron radius to be somewhat larger than the proton radius; however, the proton repulsion tends to push the protons outward and the neutron–proton force tends to pull the neutrons inward, until the
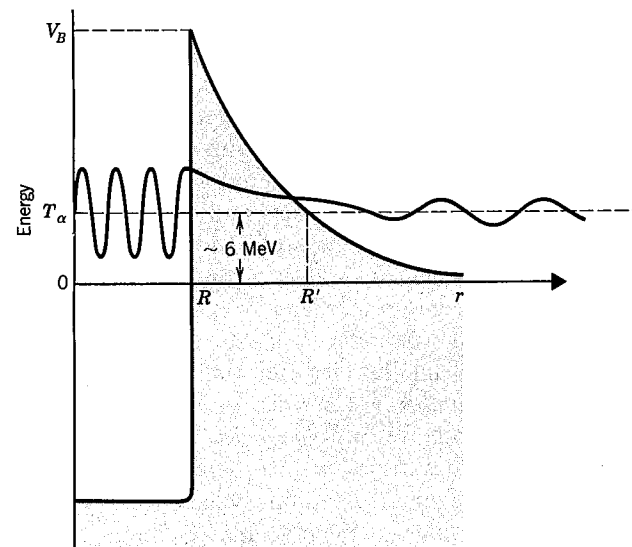
Figure 3.12 Barrier penetration in α decay. The half-life for α emission depends on the probability to penetrate the barrier, which in turn depends on its thickness. The measured half-lives can thus be used to determine the radius R where the nuclear force ends and the Coulomb repulsion begins.

neutrons and protons are so completely intermixed that the charge and matter radii are nearly equal.

3.2 MASS AND ABUNDANCE OF NUCLIDES

In Appendix C is a table of measured values of the masses and abundances of neutral *atoms* of various stable and radioactive nuclei. Even though we must analyze the energy balance in nuclear reactions and decays using nuclear masses, it is conventional to tabulate the masses of neutral atoms. It may therefore be necessary to correct for the mass and binding energy of the electrons.

As we probe ever deeper into the constituents of matter, the binding energy becomes ever greater in comparison with the rest energy of the bound system. In a hydrogen atom, the binding energy of 13.6 eV constitutes only 1.4×10^{-8} of the total rest energy of the atom. In a simple nucleus, such as deuterium, the binding energy of 2.2 MeV is 1.2×10^{-3} of the total mass energy. The deuteron is relatively weakly bound and thus this number is rather low compared with typical nuclei, for which the fraction would be more like 8×10^{-3}. At a yet deeper level, three massive quarks make up a nucleon. The masses of the quarks are not known (no free quarks have yet been confirmed experimentally and quarks may not be permitted to exist in a free state), but it is possible that they may be greater than 100 GeV/c^2. If so, the binding energy of the quarks in a nucleon would be a fraction greater than 0.99 of the total mass of the quarks— 3 quarks of total rest energy of perhaps 300 GeV combine to produce a nucleon of rest energy 1 GeV!

It is therefore not possible to separate a discussion of nuclear mass from a discussion of nuclear binding energy; if it were, then nuclei would have masses

given by $Zm_p + Nm_n$, and the subject would hardly be of interest. In this section, we confine our discussion to the experimental determination of nuclear masses, treating the nucleus as a simple object with no internal structure. In the next section we analyze the measured masses to determine the binding energy.

The measurement of nuclear masses occupies an extremely important place in the development of nuclear physics. Mass spectrometry was the first technique of high precision available to the experimenter, and since the mass of a nucleus increases in a regular way with the addition of one proton or neutron, measuring masses permitted the entire scheme of stable isotopes to be mapped. Not so with atomic physics—nineteenth-century measurements of average atomic weights led to discrepancies in the atomic periodic table, such as misordering of elements cobalt and nickel, cobalt being heavier but preceding nickel in the proper ordering based on atomic *number* not atomic *weight*. Equally as important, no understanding of nuclear structure can be successful unless we can explain the variation in nuclear properties from one isotope to another; before we can measure such properties, we must determine which isotopes are present and simultaneously attempt to separate them from one another for experimental investigations.

To determine the nuclear masses and relative abundances in a sample of ordinary matter, which even for a pure element may be a mixture of different isotopes, we must have a way to separate the isotopes from one another by their masses. The mere separation of isotopes does not require an instrument of great sensitivity—neighboring isotopes of medium-weight nuclei differ in mass by about 1%. To measure masses to precisions of order 10^{-6} requires instruments of much greater sophistication, known as *mass spectroscopes*. The separated masses may be focused to make an image on a photographic plate, in which case the instrument is called a *spectrograph*; or the masses may pass through a detecting slit and be recorded electronically (as a current, for instance), in which case we would have a *spectrometer*. A schematic diagram of a typical mass spectrograph is shown in Figure 3.13.

All mass spectroscopes begin with an *ion source*, which produces a beam of ionized atoms or molecules. Often a vapor of the material under study is bombarded with electrons to produce the ions; in other cases the ions can be formed as a result of a spark discharge between electrodes coated with the material. Ions emerging from the source have a broad range of velocities, as might be expected for a thermal distribution, and of course many different masses might be included.

The next element is a *velocity selector*, consisting of perpendicular electric and magnetic fields. The E field would exert a force qE that would tend to divert the ions upward in Figure 3.13; the B field would exert a downward force qvB. Ions pass through undeflected if the forces cancel, for which

$$qE = qvB$$

$$v = \frac{E}{B} \tag{3.19}$$

The final element is a momentum selector, which is essentially a uniform magnetic field that bends the beam into a circular path with radius r determined
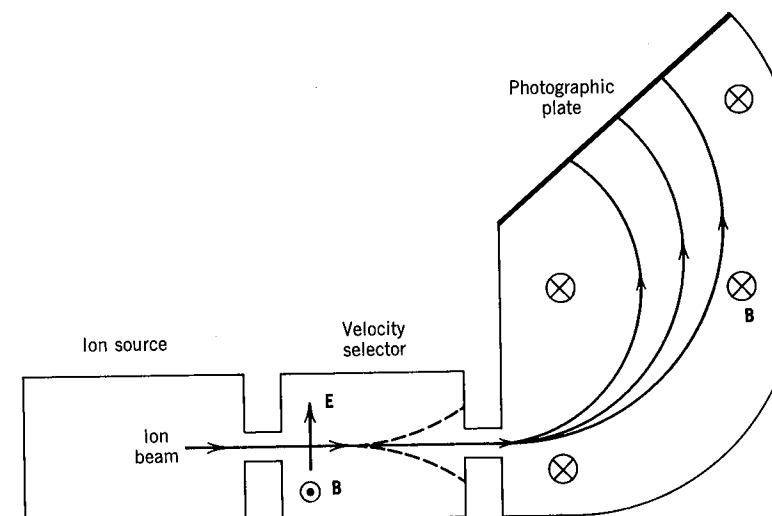
Figure 3.13 Schematic diagram of mass spectrograph. An ion source produces a beam with a thermal distribution of velocities. A velocity selector passes only those ions with a particular velocity (others being deflected as shown), and momentum selection by a uniform magnetic field permits identification of individual masses.

by the momentum:

$$mv = qBr$$

$$r = \frac{mv}{qB} \tag{3.20}$$

Since q, B, and v are uniquely determined, each different mass m appears at a particular r. Often the magnetic fields of the velocity and momentum selectors are common, in which case

$$m = \frac{qrB^2}{E} \tag{3.21}$$

To determine masses to one part in 10^6, we must know all quantities in Equation 3.21 to that precision, which hardly seems possible. In practice we could calibrate for one particular mass, and then determine all masses by relative measurements. The fixed point on the atomic mass scale is ^{12}C, which is taken to be exactly 12.000000 u. To determine the mass of another atom, such as ^1H, we would need to make considerable changes in E and B, and it is perhaps questionable whether the calibration would be valid to one part in 10^6 over such a range. It would be preferable to measure the smaller difference between two nearly equal masses. For example, let us set the apparatus for mass 128 and measure the difference between the molecular masses of C_9H_{20} (nonane) and $C_{10}H_8$ (naphthalene). This difference is measured to be $\Delta = 0.09390032 \pm 0.00000012$ u. Neglecting corrections for the difference in the molecular binding energies of the two molecules (which is of the order of 10^{-9} u), we can write

$$\Delta = m(C_9H_{20}) - m(C_{10}H_8) = 12m(^1H) - m(^{12}C)$$

Thus

$$m(^1\text{H}) = \tfrac{1}{12}\left[m(^{12}\text{C}) + \Delta\right]$$

$$= 1.00000000 + \tfrac{1}{12}\Delta$$

$$= 1.00782503 \pm 0.00000001 \text{ u}$$

Given this accurate value we could then set the apparatus for mass 28 and determine the difference between C_2H_4 and N_2:

$$\Delta = m(C_2H_4) - m(N_2) = 2m(^{12}\text{C}) + 4m(^1\text{H}) - 2m(^{14}\text{N})$$

$$= 0.025152196 \pm 0.000000030 \text{ u}$$

from which we find:

$$m(^{14}\text{N}) = m(^{12}\text{C}) + 2m(^1\text{H}) - \tfrac{1}{2}\Delta = 14.00307396 \pm 0.00000002 \text{ u}$$

This system of measuring small differences between close-lying masses is known as the *mass doublet* method, and you can see how it gives extremely precise mass values. Notice in particular how the 1 part in 10^6 uncertainties in the measured Δ values give uncertainties in the deduced atomic masses of the order of 1 part in 10^8 or 10^9.

It is also possible to determine mass differences by measuring the energies of particles in nuclear reactions. Consider the nuclear reaction $x + X \rightarrow y + Y$, in which a projectile x is incident on a stationary target X. By measuring the kinetic energies of the reacting particles, we can determine the difference in masses, which is known as the Q value of the reaction:

$$Q = \left[m(x) + m(X) - m(y) - m(Y)\right]c^2 \tag{3.22}$$

(We consider reaction Q values in detail in Section 11.2.) For example, consider the reaction $^1\text{H} + {}^{14}\text{N} \rightarrow {}^{12}\text{N} + {}^3\text{H}$. From mass doublet measurements we know that $m(^1\text{H}) = 1.007825$ u, $m(^{14}\text{N}) = 14.003074$ u, and $m(^3\text{H}) = 3.016049$ u. The measured Q value is -22.1355 ± 0.0010 MeV. We thus deduce

$$m(^{12}\text{N}) = m(^1\text{H}) + m(^{14}\text{N}) - m(^3\text{H}) - Q/c^2$$

$$= 12.018613 \pm 0.000001 \text{ u}$$

The main contribution to the uncertainty of the deduced mass comes from the Q value; the ^1H, ^3H, and ^{14}N masses are known to much greater precision. The nuclide ^{12}N is unstable and decays with a half-life of only 0.01 s, which is far too short to allow its mass to be measured with a mass spectrometer. The nuclear reaction method allows us to determine the masses of unstable nuclides whose masses cannot be measured directly.

Nuclide Abundances The mass spectrometer also permits us to measure the relative abundances of the various isotopes of an element. Measuring the current passing through an exit slit (which replaces the photographic plate of Figure 3.13) as we scan the mass range by varying E or B, we can produce results such as those shown in Figure 3.14. From the relative areas of the peaks, we can
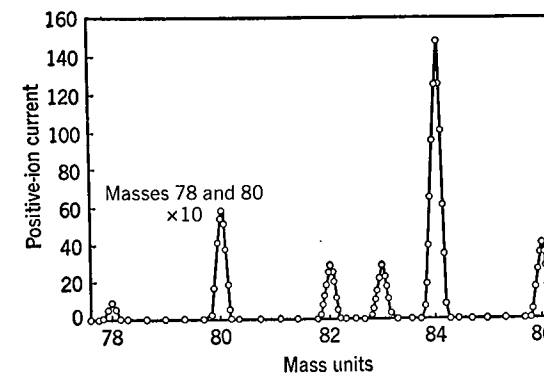
Figure 3.14 A mass-spectrum analysis of krypton. The ordinates for the peaks at mass positions 78 and 80 should be divided by 10 to show these peaks in their true relation to the others.

determine the abundances of the stable isotopes of krypton:

^{78}Kr	0.356%	^{83}Kr	11.5%
^{80}Kr	2.27%	^{84}Kr	57.0%
^{82}Kr	11.6%	^{86}Kr	17.3%

The masses that do not appear in the scan (^{79}Kr, ^{81}Kr, ^{85}Kr, plus those below ^{78}Kr and above ^{86}Kr) are radioactive and are not present in natural krypton. A typical sample of natural krypton would consist of a mixture of the six stable isotopes with the above relative composition. If we add the measured masses of the six stable isotopes with the abundances as relative weighting factors, we can compute the "average" atomic mass of krypton

$$m = 0.00356m(^{78}\text{Kr}) + 0.0227m(^{80}\text{Kr}) + \cdots$$

$$= 83.8 \text{ u}$$

which is identical with the accepted atomic mass of Kr, such as is normally given in the periodic table of the elements.

Separated Isotopes If we set the mass spectrometer on a single mass and collect for a very long time, we can accumulate a large quantity of a particular isotope, enough to use for laboratory experiments. Some mass spectrometers are designed to process large quantities of material (often at the expense of another characteristic of the equipment, such as its ability to resolve nearby masses as in Figure 3.14); the isotope separation facility at Oak Ridge National Laboratory is an example. Separated isotopes, which can be purchased from these facilities, are used for an enormous variety of experiments, not only in nuclear physics, where work with separated isotopes enables us to measure specific properties such as cross sections associated with a particular isotope, but also in other fields including chemistry or biology. For example, we can observe the ingestion of nutrients by plants using stable isotopes as an alternative to using radioactive tracers. Ordinary carbon is about 99% ^{12}C and 1% ^{13}C; nitrogen is 99.6% ^{14}N and 0.4% ^{15}N. If we surround a plant with an atmosphere of CO_2 made from
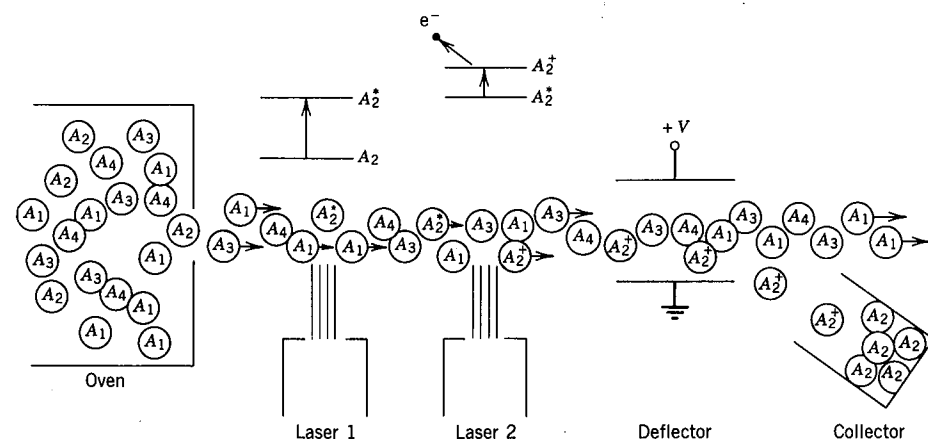
Figure 3.15 Laser isotope separation. The beam of neutral atoms from the oven is a mixture of four isotopes A_1, A_2, A_3, and A_4. The first laser is tuned to the transition corresponding to the resonant excitation of isotope A_2 to a certain excited state; because of the sharpness of the laser energy and the isotope shift that gives that particular transition a different energy in the other isotopes, only A_2 is excited. The second laser has a broad energy profile, so that many free-electron states can be reached in the ionization of the atoms; but because only the A_2 isotopes are in the excited state, only the A_2 atoms are ionized. The A_2 ions are then deflected and collected.

^{13}C, and if we use fertilizers made with ^{15}N instead of ^{14}N, we can then study how these isotopes are incorporated into the plant. The longest-lived radioactive isotope of nitrogen has a half-life of 10 min; thus, long-term studies with radioactive tracers would not be possible, and in addition radioactive decays could adversely affect the plant and the personnel who must care for them.

Laser Isotope Separation A completely different technique for separating isotopes takes advantage of the extremely sharp (that is, monochromatic) beams available from lasers. As discussed in the last section, the optical radiations of different isotopes of the same element do not have exactly the same energy; the differences in nuclear size cause small variations in the transition energies, called the *isotope shift*. Laser beams are sufficiently sharp so that they can be tuned to excite electrons in one isotope of a mixture of isotopes but not in the others. A schematic representation of the process is shown in Figure 3.15. A beam of neutral atoms passes through a laser beam, which is tuned so that electrons in the desired isotope (but not in the others) will absorb the radiation and make a transition to a particular excited state. A second laser beam is set to a wavelength that corresponds to ionization of the excited atoms. The final energy states of the free electron are continuous rather than quantized, and hence the second laser should have a broad energy profile; this will not result in the ionization of the unwanted isotopes because only those that have been excited by the first laser have electrons in the excited state. After passing through the second laser, the beam consists of ionized atoms of one isotope and neutral atoms of all the others; the ionized atoms can be removed from the beam by an electric field and collected.

3.3 NUCLEAR BINDING ENERGY

The mass energy $m_N c^2$ of a certain nuclide is its atomic mass energy $m_A c^2$ less the total mass energy of Z electrons and the total *electronic* binding energy:

$$m_N c^2 = m_A c^2 - Z m_e c^2 + \sum_{i=1}^{Z} B_i \tag{3.23}$$

where B_i is the binding energy of the ith electron. Electronic binding energies are of order 10–100 keV in heavy atoms, while atomic mass energies are of order $A \times 1000$ MeV; thus to a precision of about 1 part in 10^6 we can neglect the last term of Equation 3.23. (Even this 10^{-6} precision does not affect measurements in nuclear physics because we usually work with *differences* in mass energies, such as in determining decay or reaction energies; the effects of electron binding energies tend to cancel in these differences.)

The *binding energy* B of a nucleus is the difference in mass energy between a nucleus $^A_Z X_N$ and its constituent Z protons and N neutrons:

$$B = \left\{ Z m_p + N m_n - \left[m(^A X) - Z m_e \right] \right\} c^2 \tag{3.24}$$

where we have dropped the subscript from m_A—from now on, unless we indicate otherwise, we shall always be dealing with *atomic* masses.

Grouping the Z proton and electron masses into Z neutral hydrogen atoms, we can rewrite Equation 3.24 as

$$B = \left[Z m(^1 H) + N m_n - m(^A X) \right] c^2 \tag{3.25}$$

With the masses generally given in atomic mass units, it is convenient to include the unit conversion factor in c^2, thus: $c^2 = 931.50$ MeV/u.

We occasionally find atomic mass tables in which, rather than $m(^A X)$, what is given is the *mass defect* $\Delta = (m - A)c^2$. Given the mass defect, it is possible to use Equation 3.25 to deduce the atomic mass.

Other useful and interesting properties that are often tabulated are the neutron and proton separation energies. The *neutron separation energy* S_n is the amount of energy that is needed to remove a neutron from a nucleus $^A_Z X_N$, equal to the difference in binding energies between $^A_Z X_N$ and $^{A-1}_Z X_{N-1}$:

$$S_n = B\left(^A_Z X_N\right) - B\left(^{A-1}_Z X_{N-1}\right)$$
$$= \left[m\left(^{A-1}_Z X_{N-1}\right) - m\left(^A_Z X_N\right) + m_n \right] c^2 \tag{3.26}$$

In a similar way we can define the *proton separation energy* S_p as the energy needed to remove a proton:

$$S_p = B\left(^A_Z X_N\right) - B\left(^{A-1}_{Z-1} X_N\right)$$
$$= \left[m\left(^{A-1}_{Z-1} X_N\right) - m\left(^A_Z X_N\right) + m(^1 H) \right] c^2 \tag{3.27}$$

The hydrogen mass appears in this equation instead of the proton mass, since we are always working with *atomic* masses; you can see immediately how the Z electron masses cancel from Equations 3.26 and 3.27.

The neutron and proton separation energies are analogous to the ionization energies in atomic physics—they tell us about the binding of the outermost or

**Table 3.1** Some Mass Defects and Separation Energies

Nuclide	Δ (MeV)	S_n (MeV)	S_p (MeV)
^{16}O	−4.737	15.66	12.13
^{17}O	−0.810	4.14	13.78
^{17}F	+1.952	16.81	0.60
^{40}Ca	−34.847	15.64	8.33
^{41}Ca	−35.138	8.36	8.89
^{41}Sc	−28.644	16.19	1.09
^{208}Pb	−21.759	7.37	8.01
^{209}Pb	−17.624	3.94	8.15
^{209}Bi	−18.268	7.46	3.80

valence nucleons. Just like the atomic ionization energies, the separation energies show evidence for nuclear shell structure that is similar to atomic shell structure. We therefore delay discussion of the systematics of separation energies until we discuss nuclear models in Chapter 5. Table 3.1 gives some representative values of mass defects and separation energies.

As with many other nuclear properties that we will discuss, we gain valuable clues to nuclear structure from a *systematic* study of nuclear binding energy. Since the binding energy increases more or less linearly with A, it is general practice to show the average binding energy per nucleon, B/A, as a function of A. Figure 3.16 shows the variation of B/A with nucleon number. Several remarkable features are immediately apparent. First of all, the curve is relatively constant except for the very light nuclei. The average binding energy of most nuclei is, to within 10%, about 8 MeV per nucleon. Second, we note that the curve reaches a peak near $A = 60$, where the nuclei are most tightly bound. This suggests we can "gain" (that is, release) energy in two ways—below $A = 60$, by assembling lighter nuclei into heavier nuclei, or above $A = 60$, by breaking heavier nuclei into lighter nuclei. In either case we "climb the curve of binding energy" and liberate nuclear energy; the first method is known as *nuclear fusion* and the second as *nuclear fission*. These important subjects are discussed in Chapters 13 and 14.

Attempting to understand this curve of binding energy leads us to the *semiempirical mass formula*, in which we try to use a few general parameters to characterize the variation of B with A.

The most obvious term to include in estimating B/A is the constant term, since to lowest order $B \propto A$. The contribution to the binding energy from this "volume" term is thus $B = a_v A$ where a_v is a constant to be determined, which should be of order 8 MeV. This linear dependence of B on A is in fact somewhat surprising, and gives us our first insight into the properties of the nuclear force. If every nucleon attracted all of the others, then the binding energy would be proportional to $A(A - 1)$, or roughly to A^2. Since B varies linearly with A, this suggests that each nucleon attracts only its closest neighbors, and *not* all of the other nucleons. From electron scattering we learned that the nuclear density is roughly constant, and thus each nucleon has about the same number of neigh-
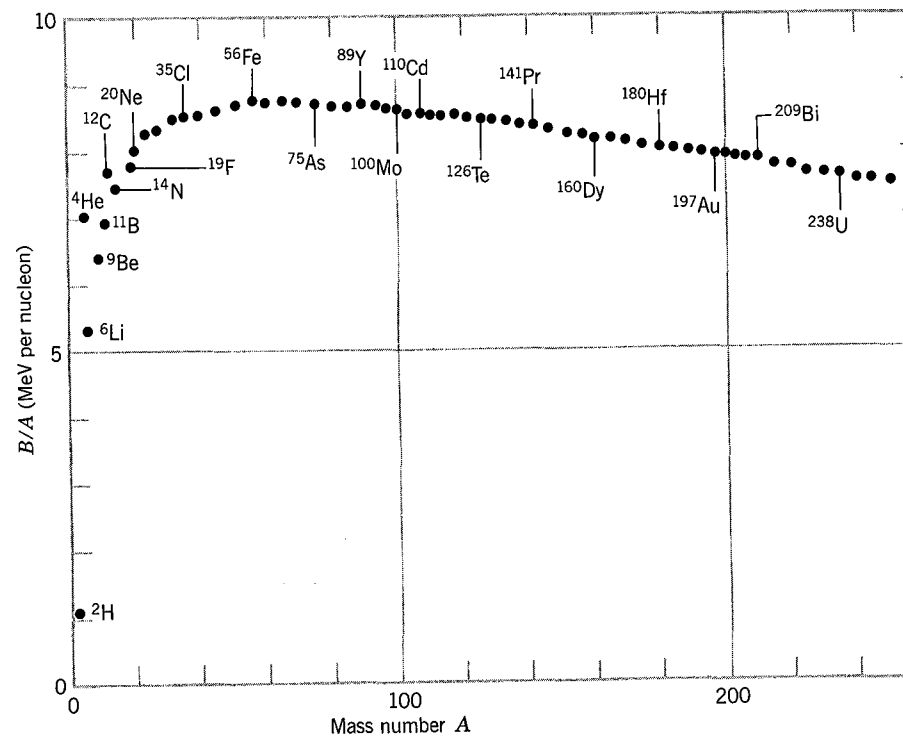
Figure 3.16 The binding energy per nucleon.

bors; each nucleon thus contributes roughly the same amount to the binding energy.

An exception to the above argument is a nucleon on the nuclear surface, which is surrounded by fewer neighbors and thus less tightly bound than those in the central region. These nucleons do not contribute to B quite as much as those in the center, and thus $B = a_v A$ overestimates B by giving full weight to the surface nucleons. We must therefore subtract from B a term proportional to the nuclear surface area. The surface area of the nucleus is proportional to R^2 or to $A^{2/3}$, since $R \propto A^{1/3}$. Thus the surface nucleons contribute to the binding energy a term of the form $-a_s A^{2/3}$.

Our binding energy formula must also include the Coulomb repulsion of the protons, which likewise tends to make the nucleus less tightly bound. Since each proton repels all of the others, this term is proportional to $Z(Z - 1)$, and we may do an exact calculation, assuming a uniformly charged sphere, to obtain $-\frac{3}{5}(e^2/4\pi\epsilon_0 R_0)Z(Z - 1)/A^{1/3}$ where the negative sign implies a reduction in binding energy. The constants evaluate to 0.72 MeV with $R_0 = 1.2$ fm; we can allow this constant to be adjustable by replacing it with a general Coulomb constant a_c.

We also note, from our study of the distribution of stable and radioactive isotopes (Figure 1.1), that stable nuclei have $Z \simeq A/2$. (The explanation for this effect will come from our discussion of the shell model in Chapter 5.) If our binding energy formula is to be realistic in describing the stable nuclei that are

actually observed, it must take this effect into account. (Otherwise it would allow stable isotopes of hydrogen with hundreds of neutrons!) This term is very important for light nuclei, for which $Z \simeq A/2$ is more strictly observed. For heavy nuclei, this term becomes less important, because the rapid increase in the Coulomb repulsion term requires additional neutrons for nuclear stability. A possible form for this term, called the symmetry term because it tends to make the nucleus symmetric in protons and neutrons, is $-a_{sym}(A - 2Z)^2/A$ which has the correct form of favoring nuclei with $Z = A/2$ and reducing in importance for large A.

Finally, we must include another term that accounts for the tendency of like nucleons to couple pairwise to especially stable configurations. When we have an odd number of nucleons (odd Z and even N, or even Z and odd N), this term does not contribute. However, when both Z and N are odd, we gain binding energy by converting one of the odd protons into a neutron (or vice versa) so that it can now form a pair with its formerly odd partner. We find evidence for this *pairing force* simply by looking at the stable nuclei found in nature—there are only four nuclei with odd N and Z (^{2}H, ^{6}Li, ^{10}B, ^{14}N), but 167 with even N and Z. This pairing energy δ is usually expressed as $+a_p A^{-3/4}$ for Z and N even, $-a_p A^{-3/4}$ for Z and N odd, and zero for A odd.

Combining these five terms we get the complete binding energy:

$$B = a_v A - a_s A^{2/3} - a_c Z(Z - 1) A^{-1/3}$$
$$- a_{sym} \frac{(A - 2Z)^2}{A} + \delta \qquad (3.28)$$

and using this expression for B we have the *semiempirical mass formula*:

$$M(Z, A) = Zm(^1H) + Nm_n - B(Z, A)/c^2 \qquad (3.29)$$

The constants must be adjusted to give the best agreement with the experimental curve of Figure 3.16. A particular choice of $a_v = 15.5$ MeV, $a_s = 16.8$ MeV, $a_c = 0.72$ MeV, $a_{sym} = 23$ MeV, $a_p = 34$ MeV, gives the result shown in Figure 3.17, which reproduces the observed behavior of B rather well.

The importance of the semiempirical mass formula is not that it allows us to predict any new or exotic phenomena of nuclear physics. Rather, it should be regarded as a first attempt to apply nuclear models to understand the systematic behavior of a nuclear property, in this case the binding energy. It includes several different varieties of nuclear models: the *liquid-drop model*, which treats some of the gross collective features of nuclei in a way similar to the calculation of the properties of a droplet of liquid (indeed, the first three terms of Equation 3.28 would also appear in a calculation of the energy of a charged liquid droplet), and the *shell model*, which deals more with individual nucleons and is responsible for the last two terms of Equation 3.28.

For constant A, Equation 3.29 represents a parabola of M vs. Z. The parabola will be centered about the point where Equation 3.29 reaches a minimum. To compare this result with the behavior of actual nuclei, we must find the minimum, where $\partial M/\partial Z = 0$:

$$Z_{min} = \frac{[m_n - m(^1H)] + a_c A^{-1/3} + 4a_{sym}}{2a_c A^{-1/3} + 8a_{sym} A^{-1}} \qquad (3.30)$$
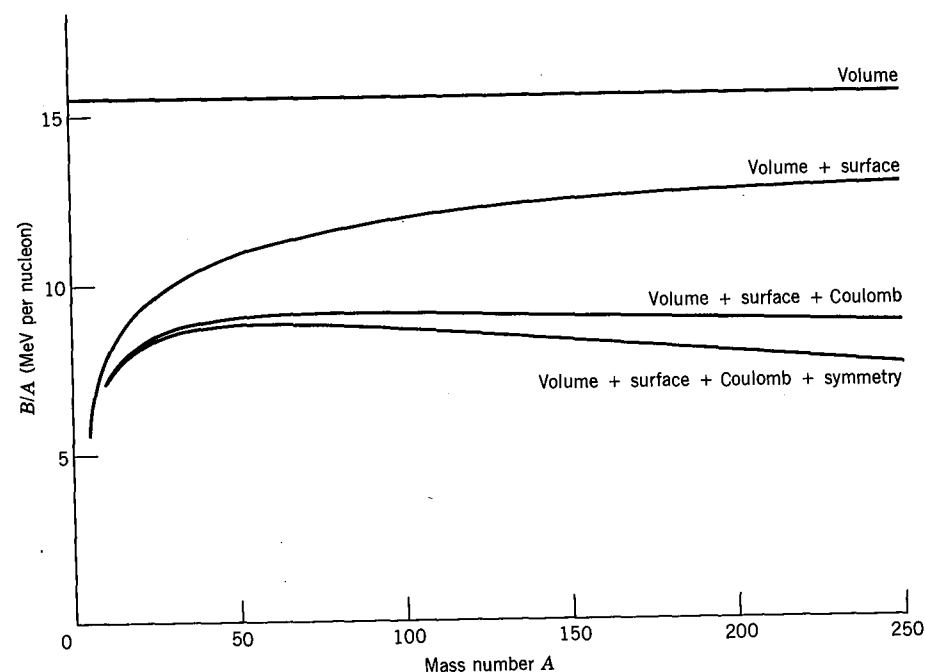
Figure 3.17 The contributions of the various terms in the semiempirical mass formula to the binding energy per nucleon.

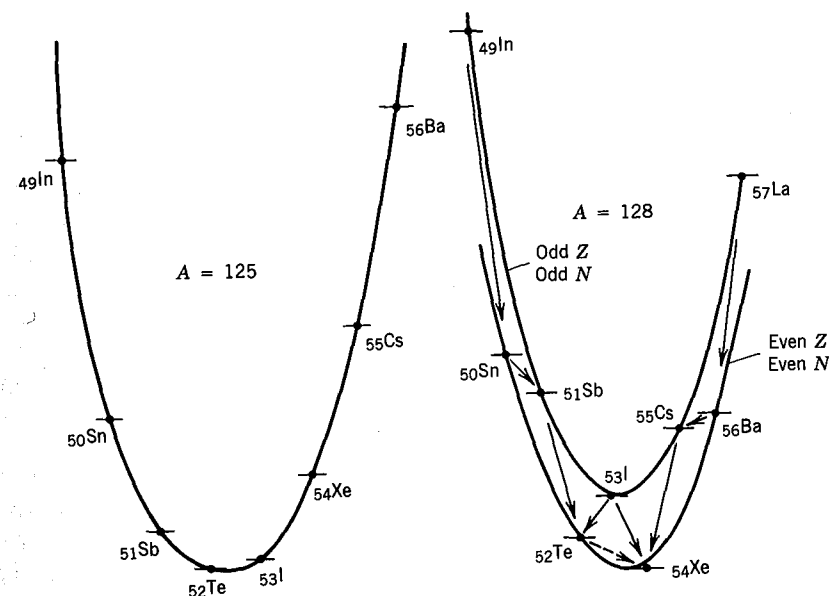**Figure 3.18** Mass chains for $A = 125$ and $A = 128$. For $A = 125$, note how the energy differences between neighboring isotopes increase as we go further from the stable member at the energy minimum. For $A = 128$, note the effect of the pairing term; in particular, ^{128}I can decay in either direction, and it is energetically possible for ^{128}Te to decay directly to ^{128}Xe by the process known as double β decay.

With $a_c = 0.72$ MeV and $a_{sym} = 23$ MeV, it follows that the first two terms in the numerator are negligible, and so

$$Z_{min} \simeq \frac{A}{2} \frac{1}{1 + \frac{1}{4}A^{2/3}a_c/a_{sym}} \tag{3.31}$$

For small A, $Z_{min} \simeq A/2$ as expected, but for large A, $Z_{min} < A/2$. For heavy nuclei, Equation 3.31 gives $Z/A \simeq 0.41$, consistent with observed values for heavy stable nuclei.

Figure 3.18 shows a typical odd-A decay chain for $A = 125$, leading to the stable nucleus at $Z = 52$. The unstable nuclei approach stability by converting a neutron into a proton or a proton into a neutron by radioactive β decay. Notice how the decay energy (that is, the mass difference between neighboring isobars) increases as we go further from stability. For even A, the pairing term gives two parabolas, displaced by 2δ. This permits two unusual effects, not seen in odd-A decays: (1) some odd-Z, odd-N nuclei can decay in either direction, converting a neutron to a proton or a proton to a neutron; (2) certain *double β decays* can become energetically possible, in which the decay may change 2 protons to 2 neutrons. Both of these effects are discussed in Chapter 9.

3.4   NUCLEAR ANGULAR MOMENTUM AND PARITY

In Section 2.5 we discussed the coupling of orbital angular momentum ℓ and spin s to give total angular momentum j. To the extent that the nuclear potential is central, ℓ and s (and therefore j) will be constants of the motion. In the quantum mechanical sense, we can therefore label every nucleon with the corresponding quantum numbers ℓ, s, and j. The total angular momentum of a nucleus containing A nucleons would then be the vector sum of the angular momenta of all the nucleons. This total angular momentum is usually called the *nuclear spin* and is represented by the symbol I. The angular momentum I has all of the usual properties of quantum mechanical angular momentum vectors: $I^2 = \hbar^2 I(I + 1)$ and $I_z = m\hbar$ ($m = -I, \ldots, +I$). For many applications involving angular momentum, the nucleus behaves as if it were a single entity with an intrinsic angular momentum of I. In ordinary magnetic fields, for example, we can observe the nuclear Zeeman effect, as the state I splits up into its $2I + 1$ individual substates $m = -I, -I + 1, \ldots, I - 1, I$. These substates are equally spaced, as in the atomic normal Zeeman effect. If we could apply an incredibly strong magnetic field, so strong that the coupling between the nucleons were broken, we would see each individual j splitting into its $2j + 1$ substates. Atomic physics also has an analogy here: when we apply large magnetic fields we can break the coupling between the electronic ℓ and s and separate the $2\ell + 1$ components of ℓ and the $2s + 1$ components of s. No fields of sufficient strength to break the coupling of the nucleons can be produced. We therefore observe the behavior of I as if the nucleus were only a single "spinning" particle. For this reason, the spin (total angular momentum) I and the corresponding spin quantum number I are used to describe nuclear states.

To avoid confusion, we will always use I to denote the nuclear spin; we will use j to represent the total angular momentum of a single nucleon. It will often

be the case that a single valence particle determines all of the nuclear properties; in that case, $I = j$. In other cases, it may be necessary to consider two valence particles, in which case $I = j_1 + j_2$, and several different resultant values of I may be possible. Sometimes the odd particle and the remaining core of nucleons each contribute to the angular momentum, with $I = j_{particle} + j_{core}$.

One important restriction on the allowed values of I comes from considering the possible z components of the total angular momentum of the individual nucleons. Each j must be half-integral ($\frac{1}{2}, \frac{3}{2}, \frac{5}{2}, \ldots$) and thus its only possible z components are likewise half-integral ($\pm\frac{1}{2}\hbar, \pm\frac{3}{2}\hbar, \pm\frac{5}{2}\hbar, \ldots$). If we have an even number of nucleons, there will be an even number of half-integral components, with the result that the z component of the total I can take only integral values. This requires that I itself be an integer. If the number of nucleons is odd, the total z component must be half-integral and so must the total I. We therefore require the following rules:

$$\text{odd-}A \text{ nuclei:} \qquad I = \text{half-integral}$$

$$\text{even-}A \text{ nuclei:} \qquad I = \text{integral}$$

The measured values of the nuclear spin can tell us a great deal about the nuclear structure. For example, of the hundreds of known (stable and radioactive) even-Z, even-N nuclei, all have spin-0 ground states. This is evidence for the nuclear pairing force we discussed in the previous section; the nucleons couple together in spin-0 pairs, giving a total I of zero. As a corollary, the ground state spin of an odd-A nucleus must be equal to the j of the odd proton or neutron. We discuss this point further when we consider the nuclear shell model in Chapter 5.

Along with the nuclear spin, the *parity* is also used to label nuclear states. The parity can take either + (even) or − (odd) values. If we knew the wave function of every nucleon, we could determine the nuclear parity by multiplying together the parities of each of the A nucleons, ending with a result π either + or −: $\pi = \pi_1 \pi_2 \cdots \pi_A$. However, in practice no such procedure is possible, for we generally cannot assign a definite wave function of known parity to every nucleon. Like the spin I, we regard the parity π as an "overall" property of the whole nucleus. It can be directly measured using a variety of techniques of nuclear decays and reactions. The parity is denoted by a + or − superscript to the nuclear spin, as I^π. Examples are 0^+, 2^-, $\frac{1}{2}^-$, $\frac{5}{2}^+$. There is no direct theoretical relationship between I and π; for any value of I, it is possible to have either $\pi = +$ or $\pi = -$.

3.5   NUCLEAR ELECTROMAGNETIC MOMENTS

Much of what we know about nuclear structure comes from studying not the strong nuclear interaction of nuclei with their surroundings, but instead the much weaker electromagnetic interaction. That is, the strong nuclear interaction establishes the distribution and motion of nucleons in the nucleus, and we probe that distribution with the electromagnetic interaction. In doing so, we can use electromagnetic fields that have less effect on the motion of nucleons than the

strong force of the nuclear environment; thus our measurements do not seriously distort the object we are trying to measure.

Any distribution of electric charges and currents produces electric and magnetic fields that vary with distance in a characteristic fashion. It is customary to assign to the charge and current distribution an electromagnetic *multipole moment* associated with each characteristic spatial dependence—the $1/r^2$ electric field arises from the net charge, which we can assign as the zeroth or *monopole* moment; the $1/r^3$ electric field arises from the first or *dipole* moment; the $1/r^4$ electric field arises from the second or *quadrupole* moment, and so on. The magnetic multipole moments behave similarly, with the exception of the monopole moment; as far as we know, magnetic monopoles either do not exist or are exceedingly rare, and thus the magnetic monopole field ($\propto 1/r^2$) does not contribute. Electromagnetic theory gives us a recipe for calculating the various electric and magnetic multipole moments, and the same recipe can be carried over into the nuclear regime using quantum mechanics, by treating the multipole moments in operator form and calculating their expectation values for various nuclear states. These expectation values can then be directly compared with the experimental values we measure in the laboratory. Techniques for measuring the nuclear moments are discussed in Chapter 16.

The simplest distributions of charges and currents give only the lowest order multipole fields. A spherical charge distribution gives only a monopole (Coulomb) field; the higher order fields all vanish. A circular current loop gives only a magnetic dipole field. Nature has not been arbitrary in the construction of nuclei; if a simple, symmetric structure (consistent with the nuclear interaction) is possible, then nuclei tend to acquire that structure. It is therefore usually necessary to measure or calculate only the lowest order multipole moments to characterize the electromagnetic properties of the nucleus.

Another restriction on the multipole moments comes about from the symmetry of the nucleus, and is directly related to the parity of the nuclear states. Each electromagnetic multipole moment has a parity, determined by the behavior of the multipole operator when $r \rightarrow -r$. The parity of electric moments is $(-1)^L$, where L is the order of the moment ($L = 0$ for monopole, $L = 1$ for dipole, $L = 2$ for quadrupole, etc.); for magnetic moments the parity is $(-1)^{L+1}$. When we compute the expectation value of a moment, we must evaluate an integral of the form $\int \psi^* \mathcal{O} \psi \, dv$, where $\mathcal{O}$ is the appropriate electromagnetic operator. The parity of ψ itself is not important; because ψ appears twice in the integral, whether $\psi \rightarrow +\psi$ or $\psi \rightarrow -\psi$ does not change the integrand. If, however, $\mathcal{O}$ has odd parity, then the integrand is an odd function of the coordinates and must vanish identically. *Thus all odd-parity static multipole moments must vanish*—electric dipole, magnetic quadrupole, electric octupole ($L = 3$), and so on.

The monopole electric moment is just the net nuclear charge Ze. The next nonvanishing moment is the *magnetic dipole moment* μ. A circular loop carrying current i and enclosing area A has a magnetic moment of magnitude $|\mu| = iA$; if the current is caused by a charge e, moving with speed v in a circle of radius r (with period $2\pi r/v$), then

$$|\mu| = \frac{e}{(2\pi r/v)}\pi r^2 = \frac{evr}{2} = \frac{e}{2m}|\ell| \qquad (3.32)$$

where $|\ell|$ is the classical angular momentum mvr. In quantum mechanics, we operationally *define* the observable magnetic moment to correspond to the direction of greatest component of ℓ; thus we can take Equation 3.32 directly into the quantum regime by replacing ℓ with the expectation value relative to the axis where it has maximum projection, which is $m_\ell \hbar$ with $m_\ell = +\ell$. Thus

$$\mu = \frac{e\hbar}{2m}\ell \qquad (3.33)$$

where now ℓ is the angular momentum quantum number of the orbit.

The quantity $e\hbar/2m$ is called a *magneton*. For atomic motion we use the electron mass and obtain the *Bohr magneton* $\mu_B = 5.7884 \times 10^{-5}$ eV/T. Putting in the proton mass we have the *nuclear magneton* $\mu_N = 3.1525 \times 10^{-8}$ eV/T. Note that $\mu_N \ll \mu_B$ owing to the difference in the masses; thus under most circumstances atomic magnetism has much larger effects than nuclear magnetism. Ordinary magnetic interactions of matter (ferromagnetism, for instance) are determined by atomic magnetism; only in very special circumstances can we observe the effects of nuclear magnetism (see Chapter 16).

We can rewrite Equation 3.33 in a more useful form:

$$\mu = g_\ell \ell \mu_N \qquad (3.34)$$

where g_ℓ is the *g factor* associated with the orbital angular momentum ℓ. For protons $g_\ell = 1$; because neutrons have no electric charge, we can use Equation 3.34 to describe the orbital motion of neutrons if we put $g_\ell = 0$.

We have thus far been considering only the orbital motion of nucleons. Protons and neutrons, like electrons, also have intrinsic or spin magnetic moments, which have no classical analog but which we write in the same form as Equation 3.34:

$$\mu = g_s s \mu_N \qquad (3.35)$$

where $s = \frac{1}{2}$ for protons, neutrons, and electrons. The quantity g_s is known as the *spin g factor* and is calculated by solving a relativistic quantum mechanical equation. For a spin-$\frac{1}{2}$ point particle such as the electron, the Dirac equation gives $g_s = 2$, and measurement is quite consistent with that value for the electron: $g_s = 2.0023$. The difference between g_s and 2 is quite small and can be very accurately computed using the higher order corrections of quantum electrodynamics. On the other hand, for free nucleons, the experimental values are far from the expected value for point particles:

$$\text{proton:} \qquad g_s = \quad 5.5856912 \pm 0.0000022$$
$$\text{neutron:} \qquad g_s = -3.8260837 \pm 0.0000018$$

(The measured magnetic moments, in nuclear magnetons, are just half the g_s factors.) Not only is the proton value far from the expected value of 2 for a point particle, but the uncharged neutron has a nonzero magnetic moment! Here is perhaps our first evidence that the nucleons are not elementary point particles like the electron, but have an internal structure; the internal structure of the nucleons must be due to charged particles in motion, whose resulting currents give the observed spin magnetic moments. It is interesting to note that g_s for the proton is greater than its expected value by about 3.6, while g_s for the neutron is

Table 3.2 Sample Values of Nuclear Magnetic Dipole Moments

Nuclide	$\mu(\mu_N)$
n	−1.9130418
p	+2.7928456
^{2}H (D)	+0.8574376
^{17}O	−1.89379
^{57}Fe	+0.09062293
^{57}Co	+4.733
^{93}Nb	+6.1705

All values refer to the nuclear ground states; uncertainties are typically a few parts in the last digit. For a complete tabulation, see V. S. Shirley, in *Table of Isotopes* (Wiley: New York, 1978), Appendix VII.

less than its expected value (zero) by roughly the same amount. Formerly these differences between the expected and measured g_s values were ascribed to the clouds of π mesons that surround nucleons, with positive and neutral π mesons in the proton's cloud, and negative and neutral π mesons in the neutron's cloud. The equal and opposite contributions of the meson cloud are therefore not surprising. In present theories we consider the nucleons as composed of three quarks; adding the magnetic moments of the quarks gives the nucleon magnetic moments directly (see Chapter 18).

In nuclei, the pairing force favors the coupling of nucleons so that their orbital angular momentum and spin angular momentum each add to zero. Thus the paired nucleons do not contribute to the magnetic moment, and we need only consider a few valence nucleons. If this were not so, we might expect on statistical grounds alone to see a few heavy nuclei with very large magnetic moments, perhaps tens of nuclear magnetons. However, no nucleus has been observed with a magnetic dipole moment larger than about $6\mu_N$.

Table 3.2 gives some representative values of nuclear magnetic dipole moments. Because of the pairing force, we can analyze these magnetic moments to learn about the nuclear structure. In Chapter 4, we discuss the magnetic moment of the deuteron, and in Chapter 5 we consider how nuclear models predict the magnetic moments of heavier nuclei.

The next nonvanishing moment is the *electric quadrupole moment*. The quadrupole moment eQ of a classical point charge e is of the form $e(3z^2 - r^2)$. If the particle moves with spherical symmetry, then (on the average) $z^2 = x^2 = y^2 = r^2/3$ and the quadrupole moment vanishes. If the particle moves in a classical flat orbit, say in the xy plane, then $z = 0$ and $Q = -r^2$. The quadrupole moment in quantum mechanics is

$$eQ = e\int \psi^*(3z^2 - r^2)\psi \, dv \qquad (3.36)$$

for a single proton; for an orbiting neutron, $Q = 0$. If $|\psi|^2$ is spherically symmetric, then $Q = 0$. If $|\psi|^2$ is concentrated in the xy plane ($z \cong 0$), then

**Table 3.3** Some Values of Nuclear Electric Quadrupole Moments

Nuclide	Q (b)
^{2}H (D)	+0.00288
^{17}O	−0.02578
^{59}Co	+0.40
^{63}Cu	−0.209
^{133}Cs	−0.003
^{161}Dy	+2.4
^{176}Lu	+8.0
^{209}Bi	−0.37

All values refer to nuclear ground states; uncertainties are typically a few parts in the last digit. For a complete tabulation, see V. S. Shirley, in *Table of Isotopes* (Wiley: New York, 1978), Appendix VII.

$Q \sim -\langle r^2 \rangle$, while if $|\psi|^2$ is concentrated along the z axis ($z \cong r$), we might have $Q \sim +2\langle r^2 \rangle$. Here $\langle r^2 \rangle$ is the mean-square radius of the orbit. Once again the pairing force is helpful, for if the paired nucleons move in spherically symmetric orbits, they do not contribute to Q. We might therefore expect that for many nuclei, the quadrupole moment can be estimated from the valence nucleon, which we can assume to orbit near the surface, so $r = R_0 A^{1/3}$. We therefore estimate $|eQ| \leq eR_0^2 A^{2/3}$, which ranges from about 6×10^{-30} em^2 for light nuclei to 50×10^{-30} em^2 for heavy nuclei. The unit of 10^{-28} m^2 is used frequently in nuclear reaction studies for cross sections, and is known as a *barn* (b). This unit is also convenient for measuring quadrupole moments; thus the expected maximum is from 0.06 to 0.5 eb. As you can see from Table 3.3, many nuclei do fall within that range, but several, especially in the rare-earth region, are far outside. Here the quadrupole moment is giving important information—the model of the single particle cannot explain the large observed quadrupole moments. Most or all of the protons must somehow collectively contribute to have such a large Q. The assumption of a spherically symmetric core of paired nucleons is not valid for these nuclei. The core in certain nuclei can take on a static nonspherical shape that can give a large quadrupole moment. The properties of such strongly deformed nuclei are discussed in Chapter 5.

3.6 NUCLEAR EXCITED STATES

Just as we learn about atoms by studying their excited states, we study nuclear structure in part through the properties of nuclear excited states. (And like atomic excited states, the nuclear excited states are unstable and decay rapidly to the ground state.) In atoms, we make excited states by moving individual electrons to higher energy orbits, and we can do the same for individual nucleons; thus the excited states can reveal something about the orbits of individual nucleons. We have already several times in this chapter referred to the complementary single-particle and collective structure of nuclei—we can also
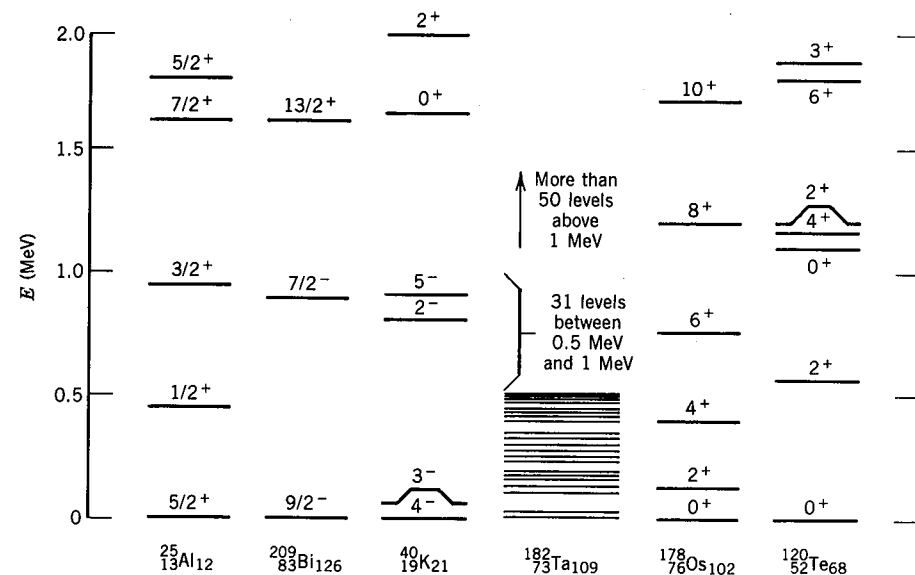
Figure 3.19 Some sample level schemes showing the excited states below 2 MeV. Some nuclei, such as ^{209}Bi, show great simplicity, while others, such as ^{182}Ta, show great complexity. There is a regularity associated with the levels of ^{178}Os that is duplicated in all even-Z, even-N nuclei in the range $150 \le A \le 190$. Structures similar to ^{120}Te are found in many nuclei in the range $50 \le A \le 150$.

produce excited states by adding energy to the core of paired nucleons. This energy can take the form of collective rotation or vibrations of the entire core, or it might even break one of the pairs, thereby adding two additional valence nucleons.

Part of the goal of nuclear spectroscopy is to observe the possible excited states and to measure their properties. The experimental techniques available include all manner of radioactive decay and nuclear reaction studies that we will consider in detail in subsequent sections. Among the properties we should like to measure for each excited state are: energy of excitation, lifetime and mode(s) of decay, spin and parity, magnetic dipole moment, and electric quadrupole moment. With more than 1000 individual nuclides, each of which may have hundreds of excited states, the tasks of measuring, tabulating, and interpreting these data are almost overwhelming.

Figure 3.19 shows some sample nuclear level schemes. A few of the excited states are identified as originating from excitations of the valence nucleons or the core; such identifications come about only after the properties listed above have been measured and have been compared with the predictions of calculations based on either single particle or collective core excitations, to see which agrees best with experiment. In subsequent chapters, we will explore the experimental techniques used to extract this information and nuclear models used to interpret it. Only through difficult and precise experiments, and through calculations involving the most powerful computers now available, can we obtain such detailed interpretations of nuclear structure.

REFERENCES FOR ADDITIONAL READING

Two essential references on nuclear charge and mass distributions are Roger C. Barrett and Daphne F. Jackson, *Nuclear Sizes and Structure* (Oxford: Clarendon, 1977), and the collection of articles on nuclear charge and moment distributions in *Atomic Data and Nuclear Data Tables* **14**, 479–653 (1974).

A collection of reprints of articles relating to electron scattering is R. Hofstadter, *Nuclear and Nucleon Structure* (New York: Benjamin, 1963). The use of muonic atoms to determine nuclear charge distributions is reviewed by C. S. Wu and L. Wilets, *Ann. Rev. Nucl. Sci*, **19**, 527 (1969). General techniques of using lasers to do high-resolution optical spectroscopy to study nuclear properties are discussed in D. E. Murnick and M. S. Feld, *Ann. Rev. Nucl. Sci.* **29**, 411 (1979). For more detail on the semiempirical mass formula, see R. D. Evans, *The Atomic Nucleus* (New York: McGraw-Hill, 1955), Chapter 11.

PROBLEMS

1. Show that the mean-square charge radius of a uniformly charged sphere is $\langle r^2 \rangle = 3R^2/5$.

2. (a) Derive Equation 3.9. (b) Fill in the missing steps in the derivation of Equation 3.13 beginning with Equation 3.9.

3. Compute the form factors $F(q)$ for the following charge distributions:
   (a) $\rho(r) = \rho_0, \quad r < R$ (b) $\rho(r) = \rho_0 \, e^{-(\ln 2) r^2 / R^2}$
   $\qquad\quad = 0, \quad r > R$

4. A nuclear charge distribution more realistic than the uniformly charged distribution is the Fermi distribution, $\rho(r) = \rho_0 \{ 1 + \exp[(r - R)/a] \}^{-1}$. (a) Sketch this distribution and compare with Figure 3.4. (b) Find the value of a if $t = 2.3$ fm. (c) What is the significance of the parameter R? (d) Evaluate $\langle r^2 \rangle$ according to this distribution.

5. Why is the electron screening correction, which is a great difficulty for analyzing electronic X rays, not a problem for muonic X rays?

6. (a) Using a one-electron model, evaluate the energies of the muonic K X rays in Fe assuming a point nucleus, and compare with the energies shown in Figure 3.8. (b) Evaluate the correction ΔE due to the finite nuclear size. Compare the corrected value with the measured energies.

7. (a) From the known masses of ^{15}O and ^{15}N, compute the difference in binding energy. (b) Assuming this difference to arise from the difference in Coulomb energy, compute the nuclear radius of ^{15}O and ^{15}N.

8. Given the following mass doublet values (in units of 10^{-6} u), compute the corresponding values for the atomic mass of ^{37}Cl:

$$m(C_3H) - m(^{37}Cl) = 41922.2 \pm 0.3$$

$$m(C_2D_8) - m(^{37}ClH_3) = 123436.5 \pm 0.1$$

$$m(C_3H_6O_2) - m(^{37}Cl_2) = 104974.24 \pm 0.08$$

Here $D \equiv {}^2H$, $C \equiv {}^{12}C$, and $O \equiv {}^{16}O$. Include in your calculation the effect of uncertainties in the H, D, O, and C masses.

9. Compute the total binding energy and the binding energy per nucleon for (a) ^{7}Li; (b) ^{20}Ne; (c) ^{56}Fe; (d) ^{235}U.

10. For each of the following nuclei, use the semiempirical mass formula to compute the total binding energy and the Coulomb energy: (a) ^{21}Ne; (b) ^{57}Fe; (c) ^{209}Bi; (d) ^{256}Fm.

11. Compute the mass defects of (a) ^{32}S; (b) ^{20}F; (c) ^{238}U.

12. Given the following mass defects, find the corresponding atomic mass: (a) ^{24}Na: -8.418 MeV; (b) ^{144}Sm: -81.964 MeV; (c) ^{240}Pu: $+50.123$ MeV.

13. Evaluate (a) the neutron separation energies of ^{7}Li, ^{91}Zr, and ^{236}U; (b) the proton separation energies of ^{20}Ne, ^{55}Mn, and ^{197}Au.

14. Examine carefully the S_n and S_p values given in Table 3.1 and draw conclusions about the strength of the binding of the last proton or neutron in the mirror pairs (^{17}O, ^{17}F) and (^{41}Ca, ^{41}Sc). Try to account for general or systematic behavior. Compare the nucleon separation energies in nuclei with identical numbers of protons or neutrons (for example, S_n in ^{16}O and ^{17}F or S_p in ^{16}O and ^{17}O). Extend these systematics by evaluating and tabulating the S_n and S_p for ^{4}He, ^{5}He, ^{5}Li and for ^{56}Ni, ^{57}Ni, and ^{57}Cu. (*Note:* Nuclei with Z or N equal to 2, 8, 20, or 28 have unusual stability. We explore the reasons for this behavior in Chapter 5.)

15. Use the semiempirical mass formula to obtain an expression for the two-neutron separation energy when $A \gg 1$. (*Hint:* A differential method is far easier than an algebraic one for this problem.) Estimate the size of the various terms and discuss the A dependence. Compare with the following data for Al and Te:

^{25}Al	31.82 MeV	^{117}Te	18.89 MeV	^{124}Te	16.36 MeV
^{26}Al	28.30 MeV	^{118}Te	18.45 MeV	^{125}Te	16.00 MeV
^{27}Al	24.42 MeV	^{119}Te	18.17 MeV	^{126}Te	15.69 MeV
^{28}Al	20.78 MeV	^{120}Te	17.88 MeV	^{127}Te	15.41 MeV
^{29}Al	17.16 MeV	^{121}Te	17.46 MeV	^{128}Te	15.07 MeV
^{30}Al	15.19 MeV	^{122}Te	17.04 MeV	^{129}Te	14.86 MeV
^{31}Al	13.03 MeV	^{123}Te	16.80 MeV	^{130}Te	14.50 MeV

Why do we choose two-neutron, rather than one-neutron, separation energies for this comparison?

16. In analogy with the previous problem, use the semiempirical mass formula to find approximate expressions for the variation of S_p with A holding Z constant. Obtain data for several sets of isotopes, plot the data, and compare with the predictions of the semiempirical mass formula.

17. The spin-parity of ^{9}Be and ^{9}B are both $\frac{3}{2}^-$. Assuming in both cases that the spin and parity are characteristic only of the odd nucleon, show how it is possible to obtain the observed spin-parity of ^{10}B (3^+). What other spin-parity combinations could also appear? (These are observed as excited states of ^{10}B.)

18. Let's suppose we can form ^{3}He or ^{3}H by adding a proton or a neutron to ^{2}H, which has spin equal to 1 and even parity. Let ℓ be the orbital angular

momentum of the added nucleon relative to the ^{2}H center of mass. What are the possible values of the total angular momentum of ^{3}H or ^{3}He? Given that the ground-state parity of ^{3}H and ^{3}He is even, which of these can be eliminated? What is the most likely value of the ground-state angular momentum of ^{3}H or ^{3}He? Can you make a similar argument based on removing a proton or a neutron from ^{4}He? (What is the ground-state spin-parity of ^{4}He?) How would you account for the spin-parity of ^{5}Li and ^{5}He ($\frac{3}{2}^-$)?

19. (a) Consider a neutron as consisting of a proton plus a negative π meson in an $\ell = 1$ orbital state. What would be the orbital magnetic dipole moment of such a configuration? Express your result as a multiple of the proton's magnetic moment. (b) Is it possible to account for the observed neutron magnetic moment from such a model? Suppose the neutron wave function consisted of two pieces, one corresponding to a $g = 0$ "Dirac" neutron and the other to proton-plus-π meson. What would be the relative sizes of the two pieces of the wave function? (Assume the proton also to behave like an ideal Dirac particle.) (c) Repeat the previous analysis for the proton magnetic moment; that is, consider the proton as part pure Dirac proton, plus part Dirac neutron with orbiting positive π meson in $\ell = 1$ state.

20. Suppose the proton magnetic moment were to be interpreted as due to the rotational motion of a positive spherical uniform charge distribution of radius R spinning about its axis with angular speed ω. (a) Show that $\mu = e\omega R^2/5$ by integrating over the charge distribution. (b) Using the classical relationship between angular momentum and rotational speed, show that $\omega R^2 = s/0.4m$. (c) Finally, obtain $\mu = (e/2m)s$, which is analogous to Equation 3.32.

21. Calculate the electric quadrupole moment of a uniformly charged ellipsoid of revolution of semimajor axis b and semiminor axis a.